



Gender difference in protein expression of vascular wall in mice exposed to chronic intermittent hypoxia: a preliminary study

Q.Y. Li^{1*}, Y. Feng^{1*}, Y.N. Lin¹, M. Li¹, Q. Guo^{1,2}, S.Y. Gu^{1,3}, J.L. Liu¹, R.F. Zhang^{1,4} and H.Y. Wan¹

¹Department of Respiratory Medicine, Ruijin Hospital, Shanghai Jiao Tong University School of Medicine, Shanghai, China

²Department of Medicine, Shanghai Dongfang Hospital, Tongji University School of Medicine, Shanghai, China

³Department of Respiratory Medicine, Shanghai Pneumology Hospital, Tongji University School of Medicine, Shanghai, China

⁴Department of Respiratory Medicine, Sir Run Run Show Hospital, Medical School of Zhejiang University, Hangzhou, Zhejiang, China

*These authors contributed equally to this study.

Corresponding authors: Q.Y. Li / H.Y. Wan

E-mail: liqingyun68@hotmail.com / hy_wan2013@163.com

Genet. Mol. Res. 13 (4): 8489-8501 (2014)

Received September 27, 2013

Accepted February 14, 2014

Published October 20, 2014

DOI <http://dx.doi.org/10.4238/2014.October.20.25>

ABSTRACT. Obstructive sleep apnea (OSA) is an independent risk factor for cardiovascular diseases such as systemic arterial hypertension, ischemic heart disease, stroke, heart failure, atrial fibrillation, and cardiac sudden death. The pathogenesis of cardiovascular disease in OSA is thought to be induced primarily by chronic intermittent hypoxia (CIH), a specific pattern of change in oxygenation during sleep. However, the underlying mechanisms of CIH-induced vasculature injury and gender differences are not well documented. The iTRAQ Quantitative Proteomic method enables analysis of a number of different proteins among several groups. Thus, we explored gender differences in protein expression in

the vascular walls of mice exposed to CIH. C57BL/6J mice of each gender were exposed to CIH with a fractional inspired O₂ (FiO₂) nadir of 5% or control, with a treatment time of 8 h/day for 28 days. Differential proteins related to CIH-induced vascular injury between genders were identified using iTRAQ proteomic technology. A total of 163 proteins were identified, of which 34 showed significant differences between genders, which may correlate with vascular injury by CIH. Twenty up-regulated proteins and 14 downregulated proteins were observed in female mice compared with male mice. We identified different vascular proteins expressed under CIH between genders, suggesting that these proteins may be biomarkers of vascular injury by CIH.

Key words: Obstructive sleep apnea; Gender difference; Vascular injury; Isobaric tag for relative and absolute quantitation; Proteomics; Chronic intermittent hypoxia

INTRODUCTION

Obstructive sleep apnea (OSA) is regarded as an independent risk factor for cardiovascular diseases such as systemic arterial hypertension, ischemic heart disease, stroke, heart failure, atrial fibrillation, and cardiac sudden death. Enhanced oxidative stress in patients with OSA has been correlated with carotid intima-media thickness (Drager et al., 2005; Kyliantreas et al., 2012) as well as coronary artery narrowing (Lu et al., 2007; Luthje and Andreas, 2008). Metabolic disorders of OSA, such as abnormal lipid metabolism (Robinson et al., 2004) and lipid peroxide-related inflammation (Lavie et al., 2004; Tan et al., 2006; Li et al., 2007), may further increase the risk of vascular diseases in OSA patients. Thus, the pathogenesis of OSA-induced vasculature injury is likely to be multifactorial and involve selective activation of inflammatory molecular pathways, endothelial dysfunction, abnormal coagulation, and abnormal lipid metabolism. Although the overall functional, structural, and biochemical alterations in vasculature have been extensively studied, the molecular mechanisms largely remain unclear.

Chronic intermittent hypoxia (CIH) induced by repetitive collapse of upper airways in OSA reflects repetitive episodes of deoxygenation followed by rapid reoxygenation. CIH leads to free radical production and increased oxidative stress, resulting in cardiovascular system injury (Schulz et al., 2000; Dyugovskaya et al., 2002). Furthermore, gender difference in the prevalence of OSAS and cardiovascular diseases have been identified in epidemiologic and clinical investigations (Young et al., 1993; Gottlieb et al., 2010), and have shown lower incidence in women. Previous studies demonstrated significant gender-dependent differences in the oxidant and antioxidant balance in mice under CIH; females showed a much higher antioxidant ability than males (Li et al., 2012). However, whether such differences exist in vascular injury under CIH remains unclear.

Proteomic analysis may be helpful for elucidating the underlying molecular mechanisms of vascular injury in OSA patients. As a quantitative proteomics study method, the isobaric tag for relative and absolute quantitation (iTRAQ) has developed as an improved approach analogous to isotope-coded affinity tags (ICAT). iTRAQ uses isotope-coded covalent tags to specifically label the N-terminus and side chain amines of peptides from protein diges-

tions, resulting in labeling of every peptide in the sample to achieve better protein identification and quantitation. In particular, the iTRAQ method can be used to compare up to 8 samples in a single experiment, providing a reliable method for reducing systematic errors (Ross et al., 2004; Chen et al., 2007; Srinivasan et al., 2012). In addition, iTRAQ combined with nano-high-performance liquid chromatography (HPLC) and tandem mass spectrometry (MS) allows for relative and absolute quantification of peptides and proteins in different samples, including clinical complex samples, organelles, and cell lysates.

In the present study, iTRAQ proteomics methods were used to identify vascular proteomics of different genders under CIH. The aim of this study was to analyze protein expression related to CIH-induced vascular injury and gender differences, which will clarify the mechanism of vascular injury by CIH.

MATERIAL AND METHODS

Animals and CIH

Twenty male and 20 female (aged 10-12 weeks) wild-type C57BL/6J mice (purchased from the Shanghai Laboratory Animal Center of the Chinese Academy of Sciences, China) were used in this study. Both female and male mice were divided into 2 groups, respectively, i.e., 10 mice in the CIH group and 10 mice in the control group. Mice in the CIH groups (10 males and 10 females) were housed in chambers to mimic sleep apnea-related CIH, i.e., the O₂ concentration inside the chamber was periodically changed between nadir fractional inspired O₂ (5%) and normal O₂ (21%) in a 90-s cycle by alternatively flushing with 100% oxygen or 100% nitrogen through computer-controlled gas valve outlets. Mice in the control groups were housed in the same device with the same valve, but flushing was conducted with compressed air rather than with oxygen and nitrogen. The treatments of both CIH and control mice were performed 8 h/day for 28 days. Ethics approval was obtained from the Ethics Committee of Ruijin Hospital.

Protein preparation and iTRAQ labeling

The eluants of protein samples from the abdominal aorta of mice were quantitated using the Bradford method. iTRAQ labeling was performed according to the kit protocol. Briefly, 100 µg proteins of each group were precipitated with cold acetone for 1 h at -20°C and resuspended in 20 µL dissolution buffer. After protein reduction and alkylation followed by overnight digestion with trypsin, the peptides were labeled with the iTRAQ reagents for 1 h at room temperature. iTRAQ reagents 114, 115, 116, and 117 were used to label the peptides from CIH male mice, control male mice, CIH female mice, and control female mice, respectively. Next, the samples were mixed, desalted using a ZipTip column, and dried in a vacuum centrifuge.

Two-dimensional (2D) liquid chromatography tandem mass spectrometry (LC-MS/MS) analysis

The iTRAQ-labeled mixed peptides were fractionated using strong cation exchange chromatography (SCX) on a 20AD HPLC system using a polysulfoethyl column. The peptide mixture was reconstituted in Buffer A (10 mM KH₂PO₄ in 25% acetonitrile, pH 2.6) and loaded

onto the column. The peptides were separated at a flow rate of 200 $\mu\text{L}/\text{min}$ for 60 min with a gradient of 0-80% Buffer B (Buffer A containing 350 mM KCl). Absorbance at 214 nm and 280 nm was monitored and a total of 20 SCX fractions were collected. The fractions were vacuum-dried and then resuspended in 50 μL HPLC Buffer A (5% acetonitrile, 0.1% formic acid), loaded onto a Zorbax 300 SB-C18 reversed-phase column, and analyzed on a QSTAR XL System coupled with a 20AD HPLC system. The flow rate of the elution was 0.3 $\mu\text{L}/\text{min}$ with gradient 5-35% HPLC Buffer B (95% acetonitrile, 0.1% formic acid) for 90 min. Survey scans were obtained with m/z ranges of 100-1800 for MS with up to 3 precursors selected from m/z 100-2000 for MS/MS.

Protein identification

Peptide mass fingerprinting (PMF) and peptide sequence spectra obtained from 4700 matrix-assisted laser desorption/ionization-time-of-flight (MALDI-TOF/TOF) were interpreted and processed using the GPS Explorer software (V3.6; Applied Biosystems; Foster City, CA, USA). The obtained MS and MS/MS spectra were then combined and submitted to the MASCOT search engine (V2.1; Matrix Science; London, UK) using the GPS Explorer software. Proteins were identified with the National Center for Biotechnology Information (NCBI) or Swiss-Prot protein database using the mouse taxonomy restriction. The spectra were further matched to proteins using the ProteinPilot software (Applied Biosystems). Next, the results obtained from different databases were compared. Other searching parameters were set as follows: MS/MS fragment tolerance was set at 0.2-0.3 Da; peptide charges were only considered to be +1; the enzyme was selected as trypsin; one missed cleavage site; no requirements for the isoelectric point and quality of protein. MS peak filtering included the following parameters: mass range 800-3000 Da, minimum S/N filter = 5, and the mass error was set as described or as slightly larger. For MS/MS peak filtering, mass range of 60 Da (parent ion mass -20 Da); the minimum S/N filter = 10; MS/MS tolerance at 0.2-0.3 Da; and the maximum number of peaks was 65 (Table 1).

Table 1. Parameters setting for protein identification.

Parameters	Settings
MS/MS tolerance	0.2-0.3 Da
Peptides charge	+1
Missed cleavage site	1
MS peak filtering mass range	800-3000 Da
MS peak filtering minimum S/N	5
MS/MS peak filtering mass range	~60 Da (parent ion mass-20 Da)
MS/MS peak filtering minimum S/N	10
MS/MS peak filtering the maximum number of peaks	65
MS/MS tolerance	0.2-0.3 Da

Data analysis

Data for differential protein expression were automatically calculated by GPS using iTRAQ. The ratios of peptide fragments among different groups were calculated. The ratio (R) was then log-transformed with a base of 1.5 ($\log_{1.5}R$). A $\log_{1.5}R$ greater than 1 or less than -1 was defined as differential expression.

RESULTS

Functional classification of proteins identified

A total of 163 proteins were identified with molecular weights ranging from 13-572 kDa. Using the online GOA software (<http://cn.expasy.org/>), 155 of the identified proteins were found to have previously identified functions, while 8 proteins had unknown functions (Table 2 and Figure 1). The molecular weights and isoelectric points of the proteins identified are shown in Figures 2 and 3.

Table 2. Functional classification of proteins identified.

Functional classification of proteins	No. of proteins
Metabolic proteins and cytoskeletal proteins	42
Protein translation and modification	36
Transcription factors	13
Nerve growth and neurotransmitter-related factor	11
Oxygen transport/oxidative stress-related proteins	9
Signal-transduction-related proteins	6
Estrogen-related proteins	2
Membrane protein and ion channel protein	6
Inflammation-related proteins	5
Renin-binding protein	1
Lipid-metabolism-related proteins	3
Cell division control-related and differentiation-related protein	5
Function-unknown proteins	8
Others	16
Total	163

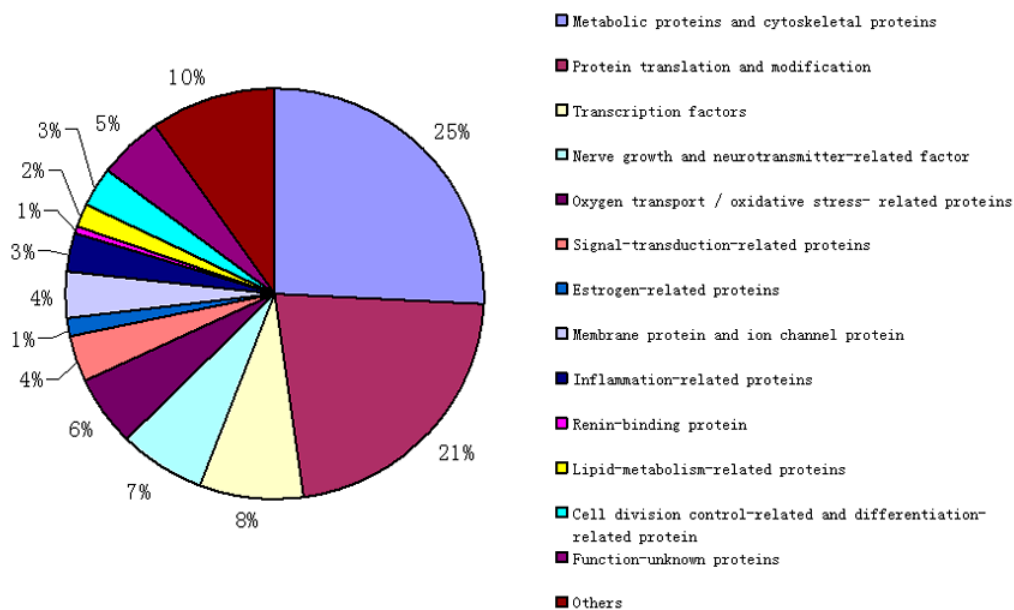


Figure 1. Functional classification of proteins identified.

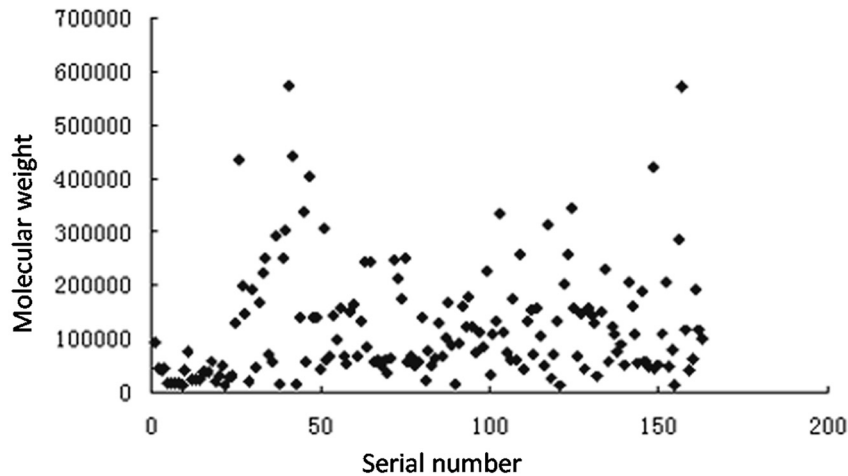


Figure 2. Scatterplot of molecular weight of proteins identified.

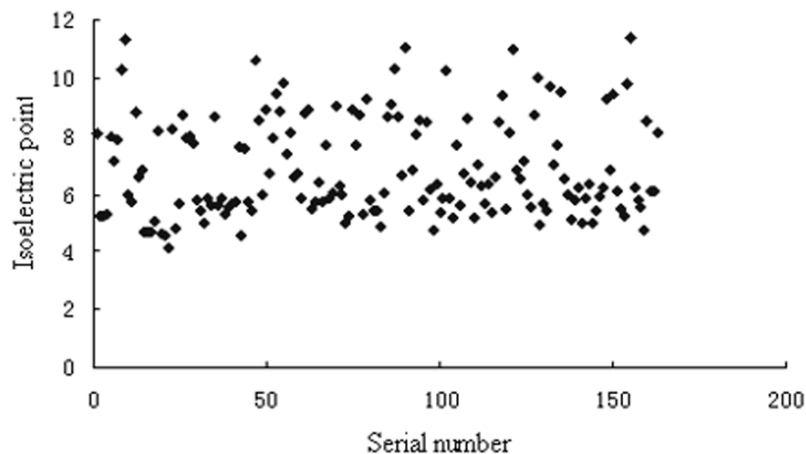


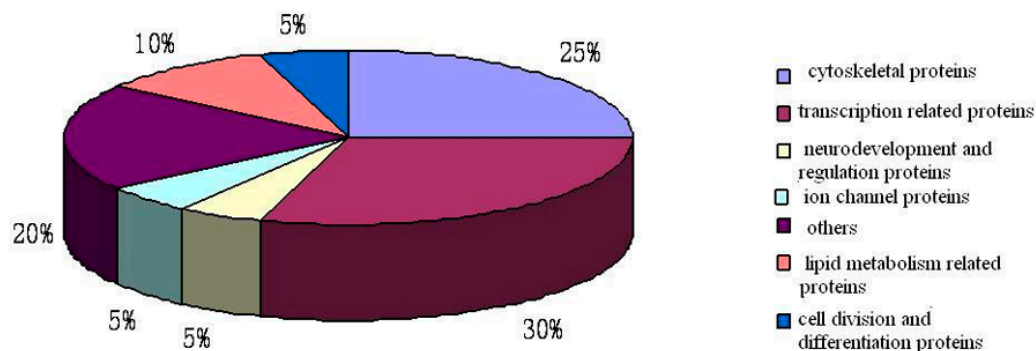
Figure 3. Scatterplot of isoelectric point of proteins identified.

Gender differences of protein expression

Thirty-four differentially expressed proteins were identified (Table 3). Among these, 20 proteins showed upregulated expression in female mice compared with males (Figure 4), including 5 cytoskeletal proteins, 6 transcription-related proteins, 1 nerve growth and neurotransmitter-related factor, 1 ion channel protein, 2 lipid metabolism-related proteins, 1 cell division control-related and differentiation-related protein, and 4 other proteins. Fourteen proteins showed downregulated expression in female mice (Figure 5), including 2 inflammation-related proteins, 3 skeleton proteins, 2 transcription-related proteins, 1 nerve growth and neurotransmitter-related factor, 1 signal-transduction-related protein, 3 unknown proteins, and 2 others.

Table 3. Identification of protein differences in abdominal aorta of different genders.

Protein name	Accession No.	log1.5*
Serum albumin precursor - <i>Mus musculus</i> (Mouse)	P07724 ALBU_MOUSE	1.55486784
Electron transfer flavoprotein subunit beta - <i>Mus musculus</i> (Mouse)	Q9DCW4 ETF_B_MOUSE	-2.168387002
Apolipoprotein A-IV precursor - <i>Mus musculus</i> (Mouse)	P06728 APOA4_MOUSE	1.086875335
Pleckstrin homology-like domain family B member 2 - <i>Mus musculus</i> (Mouse)	Q8K1N2 PHLB2_MOUSE	1.24164262
Inositol 1,4,5-trisphosphate receptor type 1 - <i>Mus musculus</i> (Mouse)	P11881 ITPR1_MOUSE	1.022918326
Decorin precursor - <i>Mus musculus</i> (Mouse)	P28654 PGS2_MOUSE	-1.172478879
Cell division control protein 6 homolog - <i>Mus musculus</i> (Mouse)	O89033 CDC6_MOUSE	1.18534042
GAS2-like protein 2 - <i>Mus musculus</i> (Mouse) plakin protein family	Q5SSG4 GA2L2_MOUSE	1.108865192
Polypeptide N-acetylgalactosaminyltransferase 2 - <i>Mus musculus</i> (Mouse)	Q6PB93 GALT2_MOUSE	1.685515304
Serine/threonine-protein kinase PCTAIRE-1 - <i>Mus musculus</i> (Mouse)	Q04735 PCTK1_MOUSE	-1.232256127
T-complex protein 1 subunit gamma - <i>Mus musculus</i> (Mouse)	P80318 TCEP_MOUSE	-1.253296803
E3 ubiquitin-protein ligase HECW2 - <i>Mus musculus</i> (Mouse)	Q616G8 HECW2_MOUSE	1.506018015
Drebrin-like protein - <i>Mus musculus</i> (Mouse)	Q62418 DBNL_MOUSE	-1.751438281
ETS translocation variant 4 - <i>Mus musculus</i> (Mouse)	P28322 ETV4_MOUSE	1.14769762
FERM, RhoGEF and pleckstrin domain-containing protein 2 - <i>Mus musculus</i> (Mouse)	Q91VS8 FARP2_MOUSE	1.14769762
Sterol O-acyltransferase 1 - <i>Mus musculus</i> (Mouse)	Q61263 SOAT1_MOUSE	1.507622819
Transcription initiation factor TFIID subunit 5 - <i>Mus musculus</i> (Mouse)	Q8C092 TAF5_MOUSE	1.215116603
Uveal autoantigen with coiled-coil domains and ankyrin repeats - <i>Mus musculus</i> (Mouse)	Q8CGB3 UACA_MOUSE	1.057915835
Serine/threonine-protein phosphatase 2B catalytic subunit alpha isoform - <i>Mus musculus</i> (Mouse)	P63328 PP2BA_MOUSE	-1.114794497
Contactin-associated protein-like 2 precursor - <i>Mus musculus</i> (Mouse)	Q9CPW0 CNTP2_MOUSE	-2.323887109
NACHT, LRR, and PYD domains-containing protein 4B - <i>Mus musculus</i> (Mouse)	Q8C6J9 NAL4B_MOUSE	-2.323887109
Zinc finger and BTB domain-containing protein 9 - <i>Mus musculus</i> (Mouse)	Q8CDC7 ZBTB9_MOUSE	1.217779991
Ubiquitin carboxyl-terminal hydrolase 19 - <i>Mus musculus</i> (Mouse)	Q3UJD6 UBP19_MOUSE	-1.007546978
Kinesin light chain 1 - <i>Mus musculus</i> (Mouse)	O88447 KLC1_MOUSE	-1.2607141
Ribosome production factor 1 - <i>Mus musculus</i> (Mouse)	Q7TND5 RPF1_MOUSE	2.213691135
Histone deacetylase 6 - <i>Mus musculus</i> (Mouse)	Q9Z2V5 HDAC6_MOUSE	-1.580308759
Leucine-rich repeats and immunoglobulin-like domains protein 1 precursor - <i>Mus musculus</i> (Mouse)	P70193 LRIG1_MOUSE	-1.007546978
Kinesin heavy chain - <i>Mus musculus</i> (Mouse)	Q61768 KINH_MOUSE	-1.000217252
Proprotein convertase subtilisin/kexin type 7 precursor - <i>Mus musculus</i> (Mouse)	Q61139 PCSK7_MOUSE	1.507622819
Abhydrolase domain-containing protein 2 - <i>Mus musculus</i> (Mouse)	Q9QXM0 ABHD2_MOUSE	1.471319497
Fanconi anemia group I protein homolog - <i>Mus musculus</i> (Mouse)	Q8K368 FANCI_MOUSE	1.465345483
Catenin alpha-3 - <i>Mus musculus</i> (Mouse)	Q65CL1 CTNA3_MOUSE	1.054513215
Protein FAM46C - <i>Mus musculus</i> (Mouse)	Q5SSF7 FA46C_MOUSE	-3.283475522
Exportin-2 - <i>Mus musculus</i> (Mouse)	Q9ERK4 XPO2_MOUSE	1.286023977
BCL-6 corepressor - <i>Mus musculus</i> (Mouse)	Q8CGN4 BCOR_MOUSE	-1.531133677

**Figure 4.** Upregulated expression proteins under chronic intermittent hypoxia (female vs male).

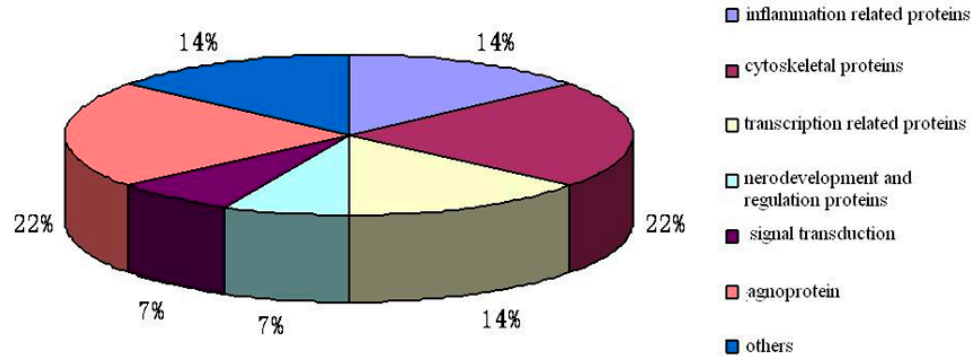


Figure 5. Downregulated expression proteins under chronic intermittent hypoxia (female vs male).

Proteins related to vascular injury

Downregulated proteins were mainly those related to inflammation, such as NACHT, LRR, and PYD domains-containing protein 4B and BCL-6 corepressor in female mice under CIH (Figures 6 and 7). Expression of lipid metabolism-related proteins was up-regulated, including apolipoprotein A-IV precursor (Figure 8) and sterol *O*-acyltransferase 1 from *Mus musculus* (Figure 9). In addition, increased expression of E3 ubiquitin-protein ligase HECW2 (Figure 10) was observed in the female group. Regarding nerve growth and regulatory proteins, pleckstrin homology-like domain family B member 2 was found to be upregulated, while contactin associated protein-like 2 precursor was found to be downregulated in female mice.

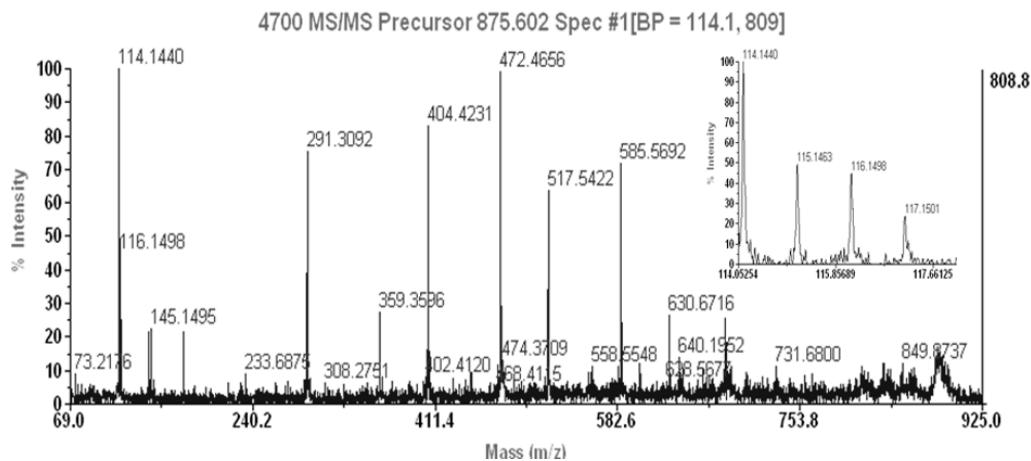


Figure 6. MS/MS spectrum of NACHT, LRR, and PYD domains-containing protein 4B.

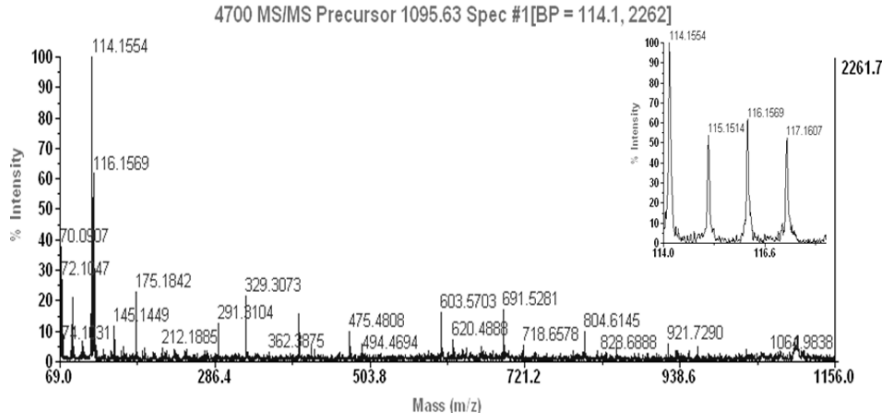


Figure 7. MS/MS spectrum of BCL-6 corepressor.

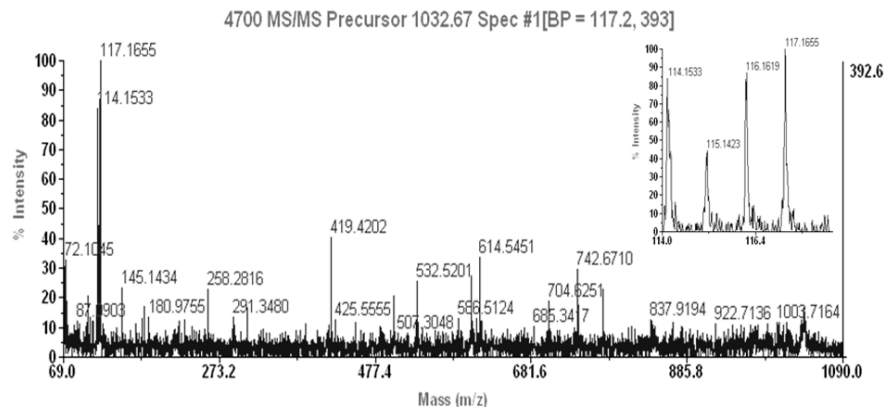


Figure 8. MS/MS spectrum of Apolipoprotein A-IV precursor.

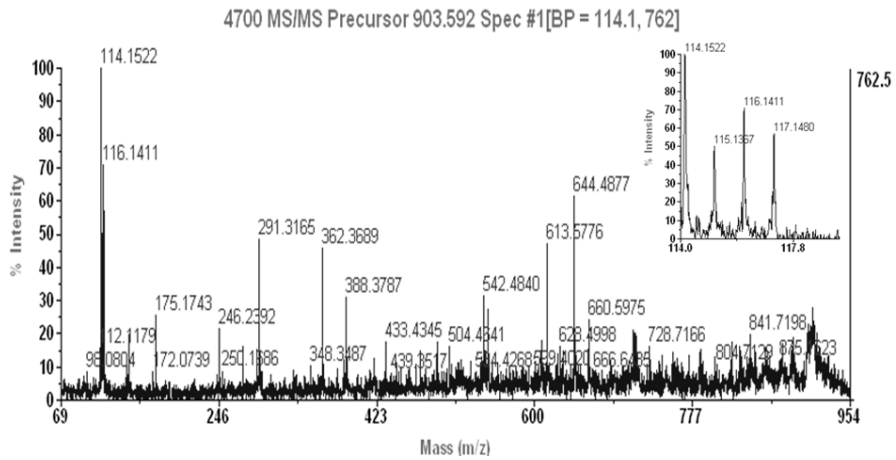


Figure 9. MS/MS spectrum of Sterol *O*-acyltransferase 1.

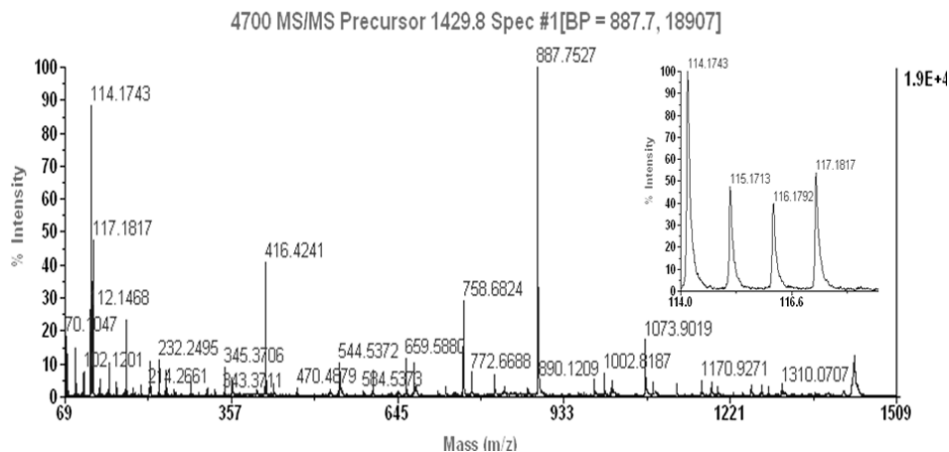


Figure 10. MS/MS spectrum of E3 ubiquitin-protein ligase HECW2.

DISCUSSION

CIH enhances oxidative stress and consequently leads to vascular injury, which involves a variety of proteins. Gender-specific expression of certain proteins was identified in this study. The proteins that may be related to the pathogenesis of vascular injury can be divided into several groups based on their functions, including inflammation-related proteins (NACHT, LRR, and PYD domains-containing protein 4B and BCL-6 corepressor), lipid metabolism-related proteins (apolipoprotein A-IV precursor and sterol *O*-acyltransferase 1 of *Mus musculus*), renin-binding protein (serine/threonine-protein kinase PCTAIRE-1), and others (ubiquitin-connection protease E3 and ETS translocation variant 4).

Inflammation-related protein, NACHT, LRR, and PYD domains-containing protein 4B, is associated with the regulation of apoptosis and pro-inflammatory factors, which takes part in systemic or local inflammation (Albrecht et al., 2003). Downregulation of this protein was observed in the vessel tissue of female mice, indicating that reduced expression of pro-inflammatory factors could play a protective role against vascular damage in female mice.

Being a member of the POZ/zinc finger (POK) family which contains an N-terminal POZ domain and 6 C-terminal zinc finger regions, BCL-6 (LAZ-3) acts as a transcription factor and has an important influence on cell survival and differentiation, particularly on lymphocytes, muscle cells, male germ cells, and keratinocytes. BCL-6 represses a number of genes involved in B cell activation and terminal differentiation, cell cycle regulation, and inflammation process related to atherosclerosis as an anti-inflammatory corepressor (Shaffer et al., 2000, Takata et al., 2008). BCL-6 corepressor is involved in BCL-6 repression, and we found that BCL-6 corepressor was downregulated, which may affect the inflammation of vascular wall in female mice under CIH.

The lipid metabolism-related protein apolipoprotein A-IV precursor (Apo A-IV) is an activator of cholesterol acyltransferase, which facilitates reverse cholesterol transport. Apo A-IV is associated with several steps of reverse cholesterol transport. Increased expression of Apo A-IV may increase the efflux of cholesterol from peripheral cells, increase esterifica-

tion of free cholesterol, and enhance CETP-mediated transfer of cholesterylesters from high-density lipoprotein to low-density lipoprotein (Deng et al., 2012). In addition, Apo A-IV has been reported to possess antioxidant-like activity. Spaulding et al. (2006) demonstrated that Apo A-IV could regulate intracellular glutathione redox balance and modulate redox-dependent apoptosis via stimulation of G-6PD activity. In our study, increased expression of Apo A-IV was observed in the vessel tissue of CIH-exposed female mice, which may partially account for the protective effects of the cardiovascular system. Acyl-CoA cholesteryl acyl transferase (ACAT) is the only intracellular enzyme that catalyzes the intracellular esterification of cholesterol and the formation of cholesteryl esters, and is thus important in cholesterol metabolism balance. ACAT also decreases cholesterol absorption, plasma cholesterol, and aortic cholesterol esterification in the aorta, and plays an important role in foam cell formation (Stein and Stein, 2005). Several medicines suppress atherosclerosis by inhibiting ACAT activity (Hsieh et al., 2012). As described above, upregulation of ACAT in the vessel tissue of CIH-exposed female mice may be another mechanism for the protective effect on the vascular system in female mice.

Nerve growth and regulatory proteins also differed between genders, such as pleckstrin homology-like domain family B member 2, contactin-associated protein-like 2, and glial fibrillary acidic protein (GFAP). According to the online GOA software, pleckstrin homology-like domain family B member 2 is involved in the assembly of the postsynaptic apparatus and aggregate acetyl-choline receptor (AChR) in the postsynaptic membrane. Expression of this protein was found to be upregulated in female mice compared with male mice and was downregulated in male mice compared with the control group. Contactin-associated protein-like 2 might play a role in forming functional distinct domains critical for saltatory conduction of nerve impulses in myelinated nerve fibers and demarcate the juxtaparanodal region of the axo-glial junction. In our study, downregulation of this protein was observed in females. GFAP, a class-III intermediate filament, is a cell-specific marker that distinguishes astrocytes from other glial cells during central nervous system development. Varying expression of this protein in the vascular wall was observed between genders, with or without CIH stimulation. CIH upregulates the expression of these proteins to varying degrees by gender, but the association of this effect with vascular injury remains unclear.

In addition, expression of N-acylglucosamine 2-epimerase was found to differ between genders. As a renin-binding protein, it catalyzes the interconversion of N-acetylglucosamine to N-acetylmannosamine and binds to renin to form a protein complex known as high-molecular weight renin, which inhibits renin activity (Park et al., 2011). Fletcher et al. (1992) found that increased renal sympathetic nerve activity was essential in hypertension development in a rat model that responds to repetitive episodic hypoxia. Levels of plasma renin activity were enhanced in the rat model and blocking the activation of angiotensin II AT1 receptors prevented the hypertension induced by CIH. Thus, IH activation of the sympathetic nervous system and the renin-angiotensin system combine to increase blood pressure. Increased plasma renin activity plays an important role in vascular injury. In our study, downregulated expression of N-acylglucosamine 2-epimerase was observed in CIH-exposed female mice, which implies that N-acylglucosamine 2-epimerase is involved in a process resulting in vascular injury.

Identification of low-abundance proteins is somewhat difficult using typical 2D electrophoresis. In our study, peptides were isolated and enriched using high-throughput 2D-nano-HPLC, a method that is reproducible and effective and offers deeper insight into tissue

proteomics, providing a basis for exploring biomarkers in vascular injury and further studies examining gender differences in the protection against vascular system injury.

In summary, we conducted a preliminary screening study on gender differential protein expression under CIH using iTRAQ proteomic methods. The proteins identified will be confirmed in subsequent studies.

ACKNOWLEDGMENTS

Research supported by the National Nature Science Foundation of China (#81070068) and by the Shanghai Nature Science Foundation (#05ZR14062).

REFERENCES

- Albrecht M, Domingues FS, Schreiber S and Lengauer T (2003). Structural localization of disease-associated sequence variations in the NACHT and LRR domains of PYPAF1 and NOD2. *FEBS Lett.* 554: 520-528.
- Chen X, Sun L, Yu Y, Xue Y, et al. (2007). Amino acid-coded tagging approaches in quantitative proteomics. *Expert Rev. Proteomics* 4: 25-37.
- Deng X, Morris J, Dressmen J, Tubb MR, et al. (2012). The structure of dimeric apolipoprotein A-IV and its mechanism of self-association. *Structure* 20: 767-779.
- Drager LF, Bortolotto LA, Lorenzi MC, Figueiredo AC, et al. (2005). Early signs of atherosclerosis in obstructive sleep apnea. *Am. J. Respir. Crit. Care Med.* 172: 613-618.
- Dyugovskaya L, Lavie P and Lavie L (2002). Increased adhesion molecules expression and production of reactive oxygen species in leukocytes of sleep apnea patients. *Am. J. Respir. Crit. Care Med.* 165: 934-939.
- Fletcher EC, Lesske J, Behm R, Miller CC III, et al. (1992). Carotid chemoreceptors, systemic blood pressure, and chronic episodic hypoxia mimicking sleep apnea. *J. Appl. Physiol.* 72: 1978-1984.
- Gottlieb DJ, Yenokyan G, Newman AB, O'Connor GT, et al. (2010). Prospective study of obstructive sleep apnea and incident coronary heart disease and heart failure: the sleep heart health study. *Circulation* 122: 352-360.
- Hsieh YH, Chen KJ, Chien SC, Cheng WL, et al. (2012). ACAT inhibitory activity of exudates from *Calocedrus macrolepis* var. *formosana*. *Nat. Prod. Commun.* 7: 1573-1574.
- Kyrintireas I, Craig S, Nethononda R, Kohler M, et al. (2012). Atherosclerosis and arterial stiffness in obstructive sleep apnea - a cardiovascular magnetic resonance study. *Atherosclerosis* 222: 483-489.
- Lavie L, Vishnevsky A and Lavie P (2004). Evidence for lipid peroxidation in obstructive sleep apnea. *Sleep* 27: 123-128.
- Li J, Savransky V, Nanayakkara A, Smith PL, et al. (2007). Hyperlipidemia and lipid peroxidation are dependent on the severity of chronic intermittent hypoxia. *J. Appl. Physiol.* 102: 557-563.
- Li QY, Li M, Feng Y, Guo Q, et al. (2012). Chronic intermittent hypoxia induces thioredoxin system changes in a gender-specific fashion in mice. *Am. J. Med. Sci.* 343: 458-461.
- Lu G, Xu ZW, Zhang YL, Yang ZJ, et al. (2007). Correlation among obstructive sleep apnea syndrome, coronary atherosclerosis and coronary heart disease. *Chin Med. J.* 120: 1632-1634.
- Luthje L and Andreas S (2008). Obstructive sleep apnea and coronary artery disease. *Sleep Med. Rev.* 12: 19-31.
- Park CS, Kim JE, Choi JG and Oh DK (2011). Characterization of a recombinant cellobiose 2-epimerase from *Caldicellulosiruptor saccharolyticus* and its application in the production of mannose from glucose. *Appl. Microbiol. Biotechnol.* 92: 1187-1196.
- Robinson GV, Pepperell JC, Segal HC, Davies RJ, et al. (2004). Circulating cardiovascular risk factors in obstructive sleep apnoea: data from randomised controlled trials. *Thorax* 59: 777-782.
- Ross PL, Huang YN, Marchese JN, Williamson B, et al. (2004). Multiplexed protein quantitation in *Saccharomyces cerevisiae* using amine-reactive isobaric tagging reagents. *Mol. Cell Proteomics* 3: 1154-1169.
- Schulz R, Mahmoudi S, Hattar K, Sibelius U, et al. (2000). Enhanced release of superoxide from polymorphonuclear neutrophils in obstructive sleep apnea. Impact of continuous positive airway pressure therapy. *Am. J. Respir. Crit. Care Med.* 162: 566-570.
- Shaffer AL, Yu X, He Y, Boldrick J, et al. (2000). BCL-6 represses genes that function in lymphocyte differentiation, inflammation, and cell cycle control. *Immunity* 13: 199-212.
- Spaulding HL, Saijo F, Turnage RH, Alexander JS, et al. (2006). Apolipoprotein A-IV attenuates oxidant-induced apoptosis in mitotic competent, undifferentiated cells by modulating intracellular glutathione redox balance. *Am. J.*

- Physiol. Cell Physiol.* 290: C95-C103.
- Srinivasan S, Thangavelu M, Zhang L, Green KB, et al. (2012). iTRAQ quantitative proteomics in the analysis of tears in dry eye patients. *Invest. Ophthalmol. Vis. Sci.* 53: 5052-5059.
- Stein O and Stein Y (2005). Lipid transfer proteins (LTP) and atherosclerosis. *Atherosclerosis* 178: 217-230.
- Takata Y, Liu J, Yin F, Collins AR, et al. (2008). PPARdelta-mediated antiinflammatory mechanisms inhibit angiotensin II-accelerated atherosclerosis. *Proc. Natl. Acad. Sci. U. S. A.* 105: 4277-4282.
- Tan KC, Chow WS, Lam JC, Lam B, et al. (2006). HDL dysfunction in obstructive sleep apnea. *Atherosclerosis* 184: 377-382.
- Young T, Palta M, Dempsey J, Skatrud J, et al. (1993). The occurrence of sleep-disordered breathing among middle-aged adults. *N. Engl. J. Med.* 328: 1230-1235.